Modelling Drug Resistant Action of tumor cells using dynamic and stochastic approaches

Sapna R * **Vijay R** **

* *Indian Institute of Technology, Madras, Chennai-600036 (e-mail: bs20b032@smail.iitm.ac.in.*
** *Indian Institute of Technology, Madras, Chennai-600036 (e-mail: be20b038@smail.iitm.ac.in.*

Abstract: Cancer treatments such as chemotherapy, radiation therapy, and combinatorial drug therapy are widely used. Despite their efficacy, cancer cells often survive due to beneficial mutations and intercellular communication. A critical component of this communication involves Tunneling nanotubules (TnTs), which facilitate the formation of complex networks among cells. Traditionally, TnTs are counted manually in research, a method susceptible to errors that can affect the consistency and reliability of experimental data.To improve this, a systems biology approach is employed to model the formation and evolution of TnT networks over time. Utilizing real-time continuous simulation allows for precise monitoring of these networks. This ensures that accurate drug concentrations are administered at the necessary times. This technique enhances the effectiveness of treatment protocols by reducing variability and increasing the accuracy of data used to determine drug dosages.

Keywords: TnTs (Tunelling Nanotubules)

1. INTRODUCTION

This project aims to create a network simulation of the behavior of a niche of tumorous cells in response to an external input (injected drug). The injected drug is modeled as a continuously spreading medium in time and space. Depending on the individual resistance of cells ,the density of the drug and the resistance of the cells in its neighborhood, the cells can either increase their resistance to the drug or die. In addition to this, the cells have the freedom to randomly move within a small lattice surrounding them.

The end goal is to monitor the resistance of these cells to the injected drug in multiple simulations and observe if the network attains a patterned structure.

2. MATERIALS AND METHODS

2.1 Model Set-up

In this model, we have assumed blood vessels to be semi-permeable hollow cylinders placed above a stack of planes containing individual cells in a lattice.

The blood vessel under consideration is aligned along the line x=0.5 parallel to the y axis and positioned at z=0.5. The cells are distributed across five planes, which are located at z=0.02, z=0.01, z=0.0, z=-0.01, and z=-0.05. The (x, y) coordinates of the cells on these planes vary from 0 to 1.

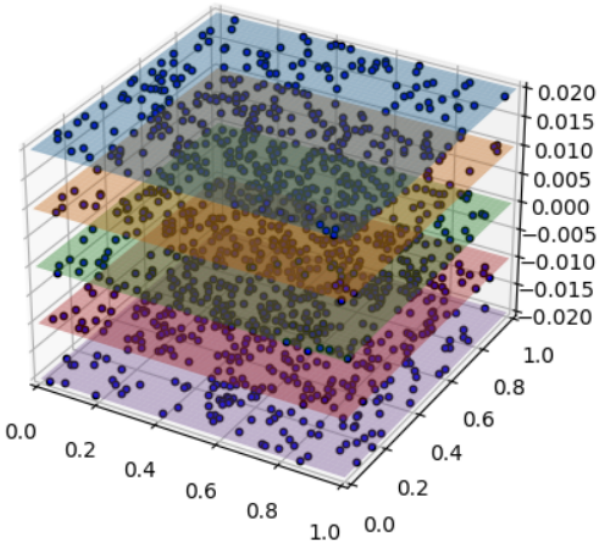

Fig. 1. Representation of the initial state of the system

The drug diffusing out of the blood vessel is modeled as a bi-variate Gaussian spreading in time and space whose equations are discussed in the upcoming sections.

The individual cells represent nodes here and the interaction between them via Tnts represent edges . The strength of the interactions are quantified by edge weights.

The formation of the edges between any two nodes is dependent on the local drug concentration, distance between the nodes and the value assigned to the individual nodes that is discussed in the upcoming sections.

Individual nodes at different spatial locations are assigned a value ranging from 0 to 1 depicting the tolerance limit of the nodes to the local drug density essentially implying that the cell dies when the local drug density is grater than the node value.

At the start of the simulation, the network is disconnected, containing 1250 nodes randomly distributed across five planes within a lattice that has a spacing of 0.01. Initially, all nodes are assigned a value of 0.26.

2.2 Overall Workflow

The overall workflow of the simulation run is presented below.

```
for i=1:simulation_time
    Update Node values
    Update lone node positions
    Spatial rewiring of connected components
    Update Edges
end
```

An Eulerian integration scheme is utilized to compute the changes in state variables at each time step.

The edgeweight between 2 connected nodes is assigned the value

$$e_{i,j} = abs(nodevalue(i) - nodevalue(j)). \tag{1}$$

The density of the drug at a certain time instant t and spatial location (x,y,z) is governed by the bivariate gaussian given below

$$D(t,x,z) = \exp\left(-\frac{(x-0.5)^2 + (z-0.5)^2}{2t^2}\right)\frac{1}{2\pi t^2} \tag{2}$$

The variance term , represented as t^2 indicates that the spread of the drug in the x-z space increases over time. The model is explicitly independent of the y component, which aligns with initial conditions specifying that the drug's distribution does not vary along the y-axis.

We will now describe the cycle consisting of four events that occur at every time step of the simulation.

2.3 Updating nodes

The nodevalues representing the resistance of individual nodes changes according to the below equation.

$$\frac{dNi}{dt} = \sigma(\mathrm{N(i)}, \mathrm{D(x,z)}) + \textstyle\sum_{j\neq i} \frac{N(j)-N(i)\cdot N_j}{\sum N(j)}. \tag{3}$$

where, σ (x,y) = x(x-y) if $D(x,z) < N(i)$ else 0.

The first term in the equation accounts for the change in the node's resistance caused by the local density of the drug. If the cell's resistance exceeds the local drug density at that instant, the drug reduces the cell's resistance, which is governed by $\sigma(N(i), D(x,z))$. A node is removed from the graph if its resistance falls below the local density of the drug, representing cell death.

The second term in the equation represents the weighted contribution from neighboring nodes through the edge weight.

Thu update of node values is followed by an instantaneous update of the edgeweights

2.4 Configurational Energy and Lone node Repositioning

The individual nodes exhibit a preference for clustering or joining connected components, as this enhances their interaction and improves their resistance to the injected drug. To model this behavior, we have defined an energy term as follows:

$$E = -\sum_{i,j\in G(k)} \frac{e_{j,i}}{r_{j,i}} \tag{4}$$

The energy of a connected component within the graph is defined as the negative summation of the ratio of edge weight $e_i i, j$ to the spatial separation $r_{i,j}$ for all edges present within the connected component.

$$E_{total} = \sum_k E(k) \tag{5}$$

The total energy of the system is the sum of the energies of individual connected components.

To facilitate the system moving towards a (local) minimal energy state, lone nodes with zero energy are permitted to randomly move within a small lattice surrounding them at each time step, enabling them to potentially join a connected component.

We have introduced two methods for the spatial rewiring of nodes within a connected component. The first method utilizes a **greedy approach**, while the second employs **simulated annealing.**

Ten simulation runs, each featuring different realizations of the model setup, were conducted for each of the methods.

2.5 Greedy Approach for connected components

The greedy method primarily aims to steer the system towards a local minimum. In this approach, a node is randomly selected from each connected component. This node is then instructed to follow a gradient descent step, moving in the direction that reduces the energy within its respective connected component.

This essentially means that the selected node moves closer to nodes with which it shares a higher edge weight. Consequently, the interaction strength is intended to increase between a more resistant node and a less resistant node, rather than between two resistant nodes or two less resistant nodes. This behavior is indicative of a disassortative network.

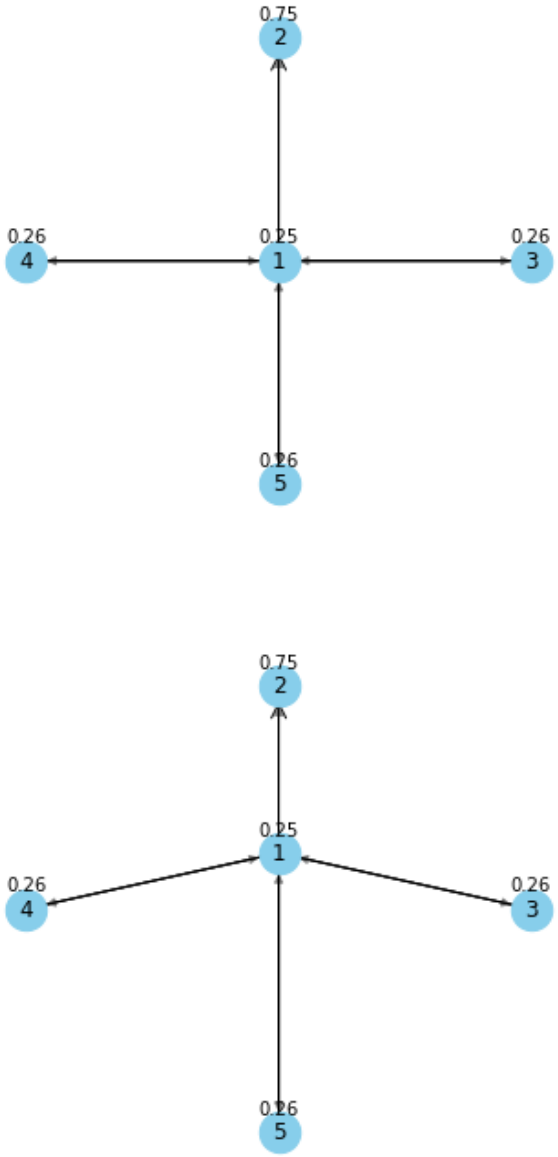

Fig. 2. Illustrating the greedy approach

As cells migrate, a notable dichotomy occurs: nodes that move closer to each other within a single timestep are likely to experience a reduction in their edge weight, as their values become more similar. Consequently, to optimize the objective of reducing energy in the subsequent timestep, the cells are likely to move in different directions.

The overall step taken by the selected node within each connected component is given by the below equation.

$$\Delta \mathbf{r_i} = 10^{-5} \sum_j \frac{e_{i,j}}{r_{i,j}^2} \hat{\mathbf{r}}_{i,j} \tag{6}$$

In the equation, j represents the neighbors of node i, and $e_{i,j}$ denotes the edge weight between node i and node j. Additionally, $\mathbf{r}_{i,j}$ is the vector pointing from node j to node i. This equation is derived by differentiating the energy equation, as described in the previous section, with respect to node i. The factor of 10^{-5} represents the learning rate in this context.

2.6 Simulated Annealing Approach for connected components

The simulated annealing approach employs a more randomized strategy, enhancing the exploration of the state space and increasing the likelihood of approaching the global minimum. At each iteration, a node is randomly selected from every connected component and permitted to move randomly within a small lattice surrounding that node.

If the movements of these selected nodes lead to a reduction in the overall energy of the system, the move is accepted. However, if the movements result in an increase in the system's energy, the moves are accepted with a probability determined by the following equation:

$$P = e^{-\frac{\Delta E}{T}} \tag{7}$$

, where T represents the temperature of the system at that iteration. We have followed a linear-ramp cooling schedule given by

$$T = 100 - \frac{t}{100}, \tag{8}$$

when t <100 and T=1, otherwise

2.7 Updating edges

To accommodate the dynamic spatial rewiring of cells described in the above sections, it's crucial to periodically update the network by inserting new edges and removing those that no longer meet the criteria due to changes in node positions and other factors.

Typically, nodes with identical resistance values do not connect, as their edge weights are essentially zero. Additionally introducing spatial constraints to mimic the biological environment allows for interaction via tunneling nanotubes (Tnts) only if the nodes are within a specific distance threshold.

In our model, we have incorporated these factors, setting the maximum separation allowed for edge formation between two nodes at 0.04 units.

Thus,edges form between two nodes if the separation distance $r_{i,j} < 0.04$ units and the potential edgeweight formed by the nodes ,represented by $e_{i,j} > 0$ Similarly 2 nodes break off their edge if their seperation distance is $>$ 0.05 units

These constraints ensures that only nodes within a certain distance threshold can potentially stay in a connection, aligning with the spatial realism of the system.

3. RESULTS AND DISCUSSION

The results from conducting 10 different simulations using the Greedy and Simulated Annealing approaches for spatial rewiring are presented in the Figures section.

Figures on the left show results from simulations using the Greedy approach for spatial rewiring.

Figures on the right display results from simulations where the Simulated Annealing approach was employed for spatial rewiring.

3.1 Configurational Energy

Upon comparing Figure 3 and Figure 6, it is evident that both strategies guide the system towards a minimum. However, a significant difference is observed in the scale of the y-values on the y-axis, which represent the system's energy. The Greedy approach results in more than a 20-fold reduction in energy compared to the Simulated Annealing approach. This suggests that the final state of the system achieved using the Greedy strategy is likely to be more closely clustered compared to the state resulting from the Simulated Annealing approach.

3.2 Number of Survivimg Cells

It is clear that the survival of cells following a drug attack is almost exclusively dependent on drug diffusion, as demonstrated by the nearly identical curves presented in Figures 4 and 7.

3.3 Fraction of Lone Nodes

The fraction of lone nodes decreases from 1 to 0, primarily due to the elimination of many lone nodes by the drug attack and the high likelihood of these nodes joining other connected components. Figures 5 and 8 show nearly identical curves, suggesting that the primary factor driving this reduction is the drug attack.

3.4 Node Value Distribution

The node value distribution histograms in Fig 9. and Fig 12. is skewed towards the right indicating that most of the surviving nodes/cells have become super resistant to future attack.

3.5 Degree Distribution

Upon comparing Figures 10 and 13, it's apparent that the Greedy approach has resulted in a graph with a greater number of high-degree nodes (maximum degree=8), whereas the outcome from the Simulated Annealing approach features a histogram more populated around degrees 3 and 4.

3.6 Final State of the Networks

The average number of surviving cells using the Greedy and Simulated Annealing approaches are 125 and 113, respectively. Observations from Figures 11 and 14 reveal that the Greedy approach results in a more closely clustered system, while the Simulated Annealing approach produces a system that is more dispersed in the z-direction. In both scenarios, all nodes that were initially located in the middle of the planes have been eliminated due to the drug attack.

4. CONCLUSION AND FUTURE STUDIES

The current model minimally incorporates biological factors, assuming nearly ideal conditions for passive drug diffusion and a homogeneous diffusion medium. Additionally, it does not account for the time drugs take to pass through the lipid transmembrane layers of cell membranes, entering the cell interior. Consequently, the results discussed here may not directly correlate with actual drug dosages.

To enhance the model's relevance and accuracy, integrating more comprehensive biological constraints could yield results that more closely mimic real cellular environments. For instance, one immediate improvement could be to introduce variability in the initial resistance of nodes instead of maintaining uniformity. This adjustment allows the system to begin forming interactions even before the drug diffuses, facilitating the modeling of delayed drug responses and other dynamic interactions within the system.

5. CODE AND DATA AVAILABILITY

The code utilized in developing this project is accessible here. The data for the project was generated internally using the ‘networkx‘ and ‘numpy‘ packages.

6. ACKNOWLEDGEMENT

We thank Dr Karthik Raman, for providing us this opportunity to build our project. We also thank the Tas for their constant support.

7. REFERENCES

1. Ceran Y, Ergüder H, Ladner K, Korenfeld S, Deniz K, Padmanabhan S, Wong P, Baday M, Pengo T, Lou E, et al. TNTdetect.AI: A Deep Learning Model for Automated Detection and Counting of Tunneling Nanotubes in Microscopy Images. Cancers. 2022; 14(19):4958. https://doi.org/10.3390/cancers14194958

2. Hodneland E, Lundervold A, Gurke S, Tai XC, Rustom A, Gerdes HH. Automated detection of tunneling nanotubes in 3D images. Cytometry A. 2006 Sep 1;69(9):961-72. doi: 10.1002/cyto.a.20302. PMID: 16969816.

3.Ottonelli I, Caraffi R, Tosi G, Vandelli MA, Duskey JT, Ruozi B. Tunneling Nanotubes: A New Target for Nanomedicine? Int J Mol Sci. 2022 Feb 17;23(4):2237. doi: 10.3390/ijms23042237. PMID: 35216348; PMCID: PMC8878036.

4.Dupont M, Souriant S, Lugo-Villarino G, Maridonneau-Parini I and Vérollet C (2018) Tunneling Nanotubes: Intimate Communication between Myeloid Cells. Front. Immunol. 9:43. doi: 10.3389/fimmu.2018.00043

5. Bravo-Cordero JJ, Hodgson L, Condeelis J. Directed cell invasion and migration during metastasis. Curr Opin Cell Biol. 2012 Apr;24(2):277-83. doi: 10.1016/j.ceb.2011.12.004. Epub 2011 Dec 30. PMID: 22209238; PMCID: PMC3320684.

6. Chen J, Sprouffske K, Huang Q, Maley CC (2011) Solving the Puzzle of Metastasis: The Evolution of Cell Migration in Neoplasms. PLoS ONE 6(4): e17933. https://doi.org/10.1371/journal.pone.0017933

8. FIGURES

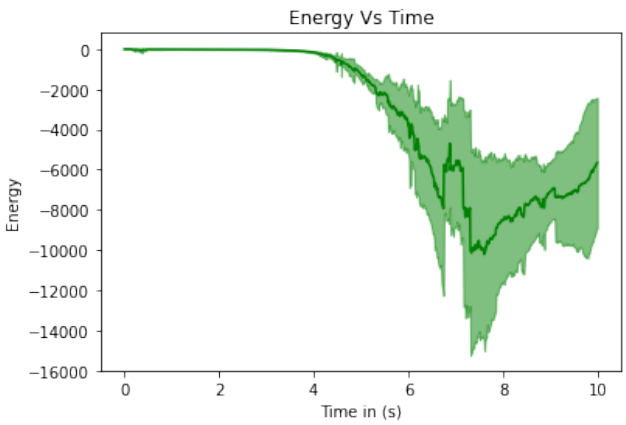

Fig. 3. Configurational Energy in time Greedy Approach

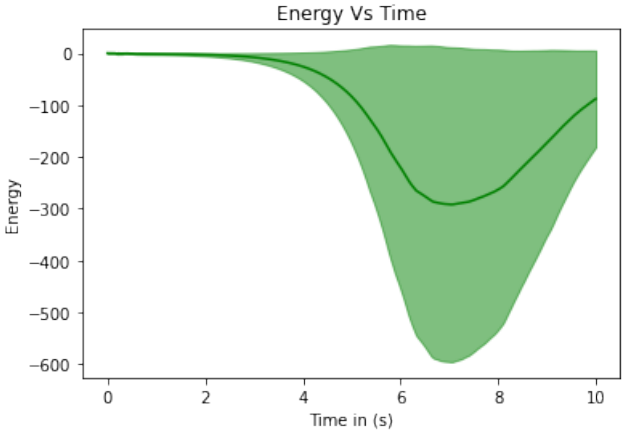

Fig. 6. Configurational Energy in time Simulated Annealing Approach

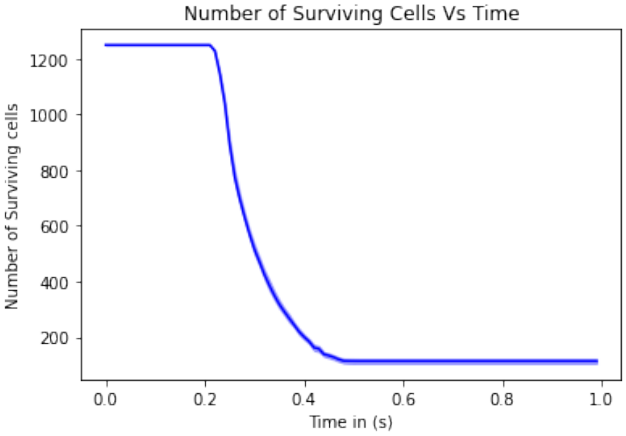

Fig. 4. Number of surviving cells using the greedy approach

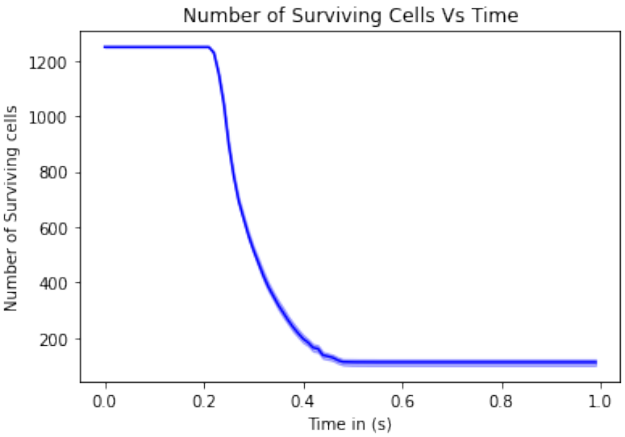

Fig. 7. Number of surviving cells using the Simulated Annealing

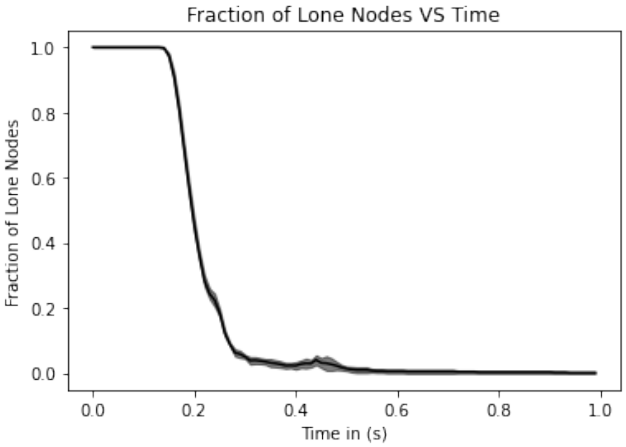

Fig. 5. Fraction of lone nodes using greedy approach

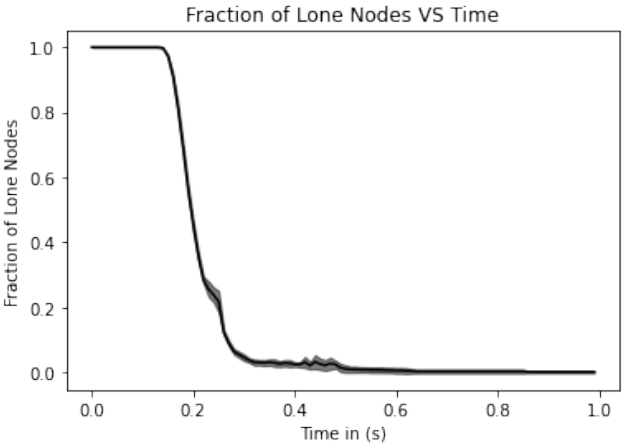

Fig. 8. Fraction of lone nodes using Simulated Annealing

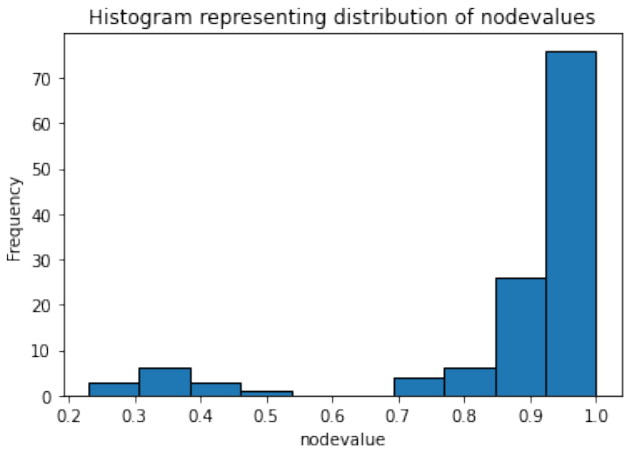

Fig. 9. Node value Distribution obtained using Greedy Approach

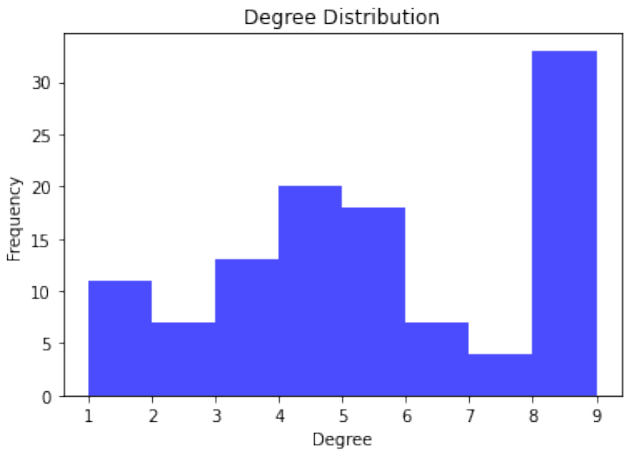

Fig. 10. Degree Distribution obtained using Greedy Approach

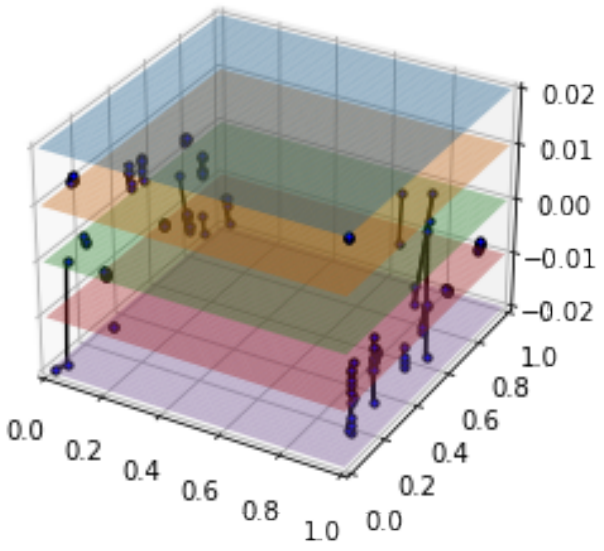

Fig. 11. Final State of the network using Greedy Approach

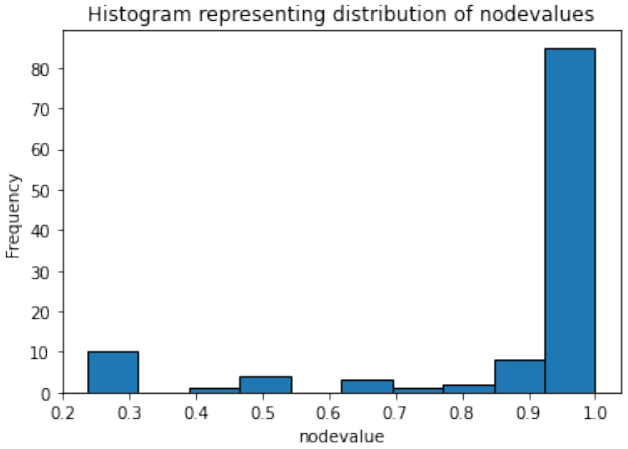

Fig. 12. Node value Distribution obtained using Simulated Annealing Approach

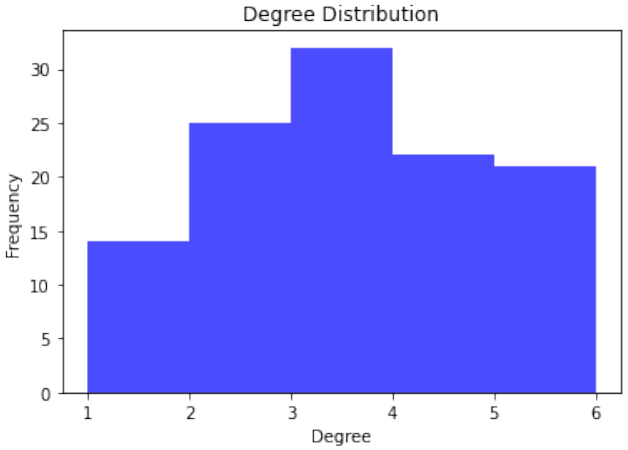

Fig. 13. Degree Distribution obtained using Simulated Annealing Approach

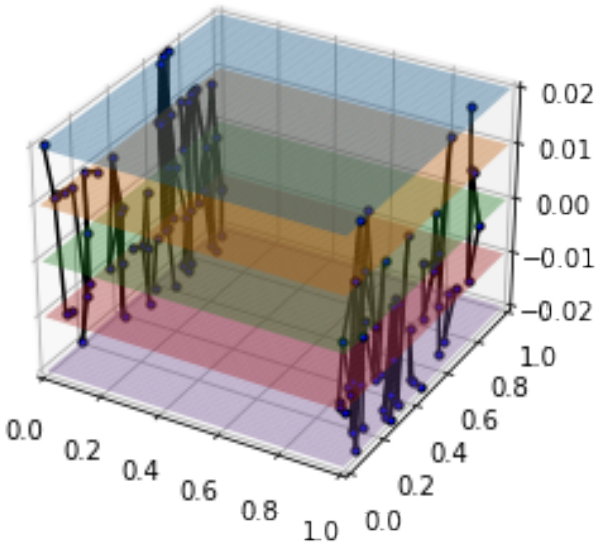

Fig. 14. Final State of the network using Simulated Annealing Approach